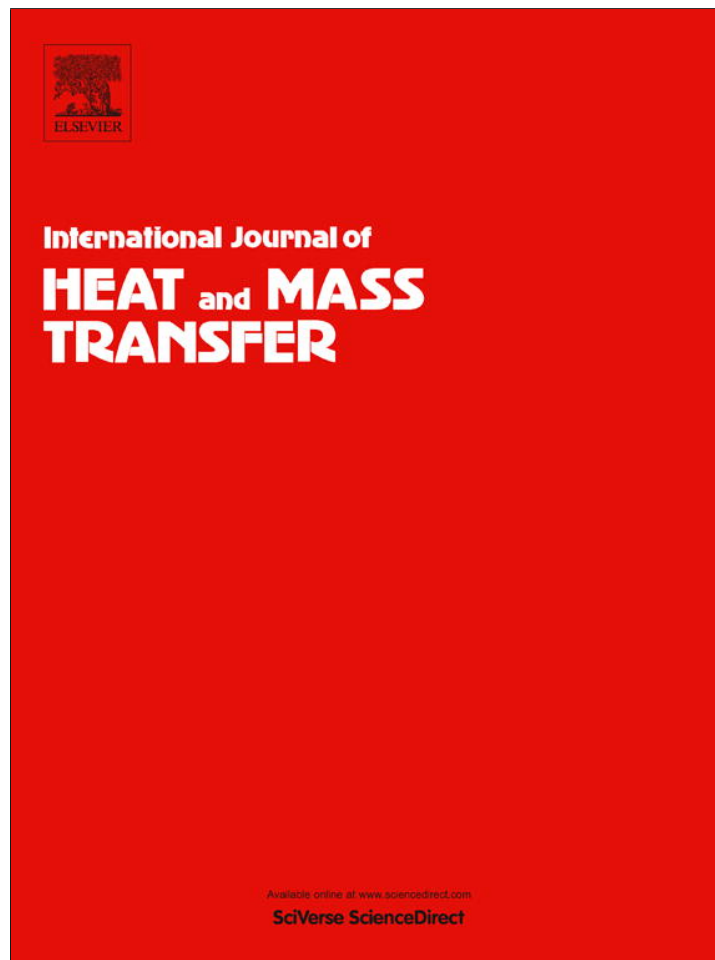


Provided for non-commercial research and education use.
Not for reproduction, distribution or commercial use.



(This is a sample cover image for this issue. The actual cover is not yet available at this time.)

This article appeared in a journal published by Elsevier. The attached copy is furnished to the author for internal non-commercial research and education use, including for instruction at the authors institution and sharing with colleagues.

Other uses, including reproduction and distribution, or selling or licensing copies, or posting to personal, institutional or third party websites are prohibited.

In most cases authors are permitted to post their version of the article (e.g. in Word or Tex form) to their personal website or institutional repository. Authors requiring further information regarding Elsevier's archiving and manuscript policies are encouraged to visit:

<http://www.elsevier.com/copyright>



Contents lists available at SciVerse ScienceDirect

International Journal of Heat and Mass Transfer

journal homepage: www.elsevier.com/locate/ijhmt

Fundamental investigation of fluidic optical devices: Transmission characteristics of laser beam in 1D temperature field of liquid medium

Hong Duc Doan ^{*}, Kazuyoshi Fushinobu, Ken Okazaki

Tokyo Institute of Technology, Box 16-3, Meguro-ku, Tokyo 152-8550, Japan

ARTICLE INFO

Article history:

Received 1 February 2012

Received in revised form 18 December 2012

Accepted 20 December 2012

Keywords:

Thermal lens effect

Temperature distribution

Refractive angle

ABSTRACT

Laser measurement and laser processing techniques have been gaining strong attention from various applications. This research aims at the development of a novel optical device, and in order to fulfill the objective, characteristics of the thermal lens effect is studied. This phenomenon has the optical property of a divergent lens since the refractive index distribution on the optical axis is formed when the liquid medium is irradiated. One reason for the refractive index distribution is the temperature distribution in the liquid medium when it is irradiated. In this research, as a fundamental step to develop the fluidic optical devices, the interaction between a refractive angle of the probe beam and the temperature distribution on the thermal lens effect is investigated.

© 2012 Elsevier Ltd. All rights reserved.

1. Introduction

Gordon et al. [1] reported that the beam shape of incident laser light expands after passing through a liquid medium. This phenomenon was termed “the thermal lens effect,” and it has become a well-known photo-thermal phenomenon. Phenomenological, optical, and spectroscopic studies of the thermal lens effect have been carried out to describe nonlinear defocusing effect [2–8]. Recent progress in laser technology has revealed the various aspects of the thermal lens effect. Based on these efforts, other mechanisms, such as liquid density, electronic population, and molecular orientation, have been found to play important role as well as thermal lens effect. Recent studies term these effects as “the transient lens effect” [9,10]. The main advantage of using the transient lens effect in Photo-thermal-spectroscopy is that the sensitivity is 100–1000 greater than a traditional absorptiometry [11].

In this research, a new idea of applying the thermal lens effect to develop fluidic optical device is proposed. A schematic of the concept is shown in Fig. 1. The rectangular solid region in Fig. 1a represents the liquid medium, which has a temperature field created by a heater-heat sink system or laser-induced absorption. By controlling the temperature field as well as refractive index distribution of liquid medium, the refractive angle of each light ray passing through the liquid medium can be controlled in order to develop fluidic optical devices such as: optical switching in

Fig. 1a, beam shaper in Fig. 1b and lens in Fig. 1c. Merits of these devices include flexibility of optical parameters, versatility and low cost.

In this research, as a first step to develop fluidic optical device, the refractive characteristics of a probe beam, which is transmitted in one-dimensional temperature distribution in a liquid sample is studied.

2. Basics of the light ray transmitted in one-dimensional refractive index liquid sample

In this research, the light ray is modeled in the domain shown in Fig. 2, to calculate the refractive angle of the probe beam, which is transmitted in a one-dimensional temperature distribution in the liquid medium. The light ray direction transmitted in a medium having a refractive index dependent only on the y -axis, is described by the following form [12]

$$x = \int_0^y \frac{n_0 \sin \theta \cos \varphi}{\sqrt{n^2(y) - n_0^2 \sin^2 \theta}} dy \quad (1)$$

$$z = \int_0^y \frac{n_0 \sin \theta \sin \varphi}{\sqrt{n^2(y) - n_0^2 \sin^2 \theta}} dy \quad (2)$$

In which, the light ray passes through the medium at coordinate center, θ and φ are the incident angle with y - and x -axis respectively, n_0 is the refractive index of the liquid medium at the coordinate center.

^{*} Corresponding author. Tel./fax: +81 03 5734 2500.

E-mail address: doan.d.aa@m.titech.ac.jp (H.D. Doan).

Nomenclature

a	Thermal diffusivity, m^2/s
d	Distance from the sample to the detector of the CCD camera, m
g	Acceleration of gravity, m/s^2
L	Thickness of liquid medium, m
n	Refractive index of the liquid medium
n_0	Refractive index at coordinate center
r	Central position of the probe beam, mm
R	Positional vector of the light ray
T	Temperature, K
x, y, z	Cartesian coordinate, m

v, w Velocity in y, z directions, m/s

Greek symbols

θ	Incident angle with the y -axis, rad
φ	Incident angle with the x -axis, rad
α	Refractive angle, rad
β	Angle between the y -axis and ray direction vector, rad
γ	Angle between the z -axis and ray direction vector, rad
λ	Probe beam wavelength, nm
Φ	Beam waist, mm

3. Theoretical modeling

Fig. 2 shows a schematic diagram of the model set up. The rectangular solid medium in the figure represents the domain considered in the calculation which consists of ethylene glycol. In the medium, ethylene glycol has linear temperature distribution in only the y -axis direction and the probe beam propagate along z -axis direction. Therefore, $\theta = \varphi = \pi/2$, and Eqs. 1 and 2 become:

$$x = 0 \tag{3}$$

$$z = \int_0^y \frac{n_0}{\sqrt{n^2(y) - n_0^2}} dy \tag{4}$$

The temperature distribution of the liquid medium is modeled with a linear function of the variable y and temperature T at point y is calculated following:

$$T(y) = T_0 + \frac{dT}{dy}y \tag{5}$$

In which, T_0 is the temperature of the liquid medium at coordinate origin and dT/dy is constant.

Furthermore, between 0 and 100 °C refractive index of ethylene glycol is a linear function of temperature with refractive index change $dn/dT = -2.6 \times 10^{-4} K^{-1}$ [13]. Therefore, the relationship between refractive index and the variable y can be rewritten following:

$$y = \frac{n(y) - n_0}{dn/dy} \tag{6}$$

and

$$dy = dn \times \frac{dy}{dn} = dn \times \frac{dy}{dT} \times \frac{dT}{dn} = \frac{dn}{k} \tag{7}$$

where,

$$k = -2.6 \times 10^{-4} \times \frac{dT}{dy} \tag{8}$$

By substituting Eq. (7) into Eq. (4) and solving the differential equation, the relationship between y and z can be obtained following:

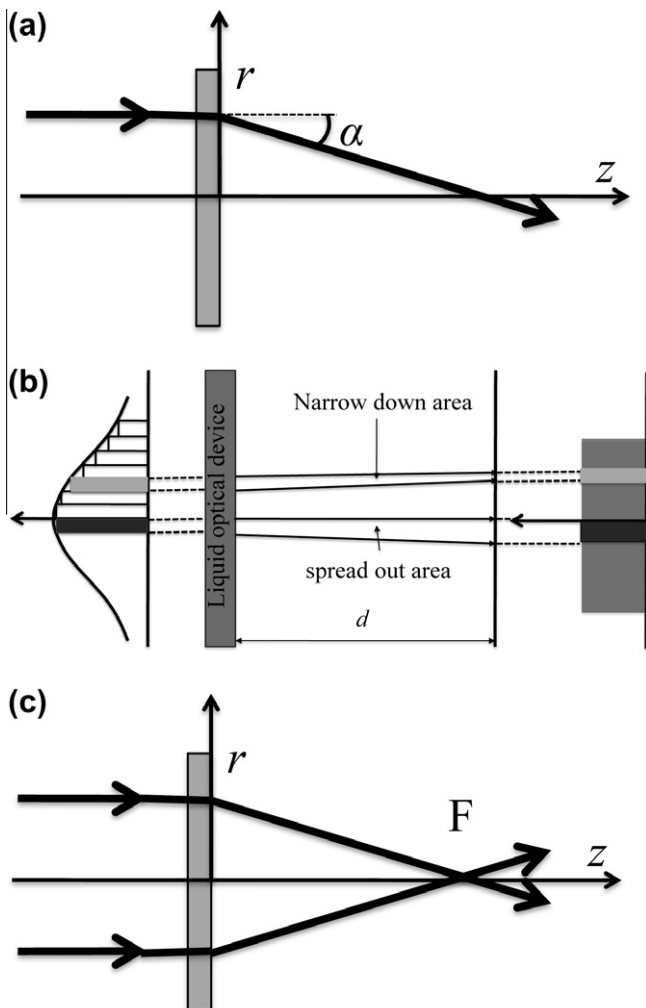


Fig. 1. Image of fluidic optical devices.

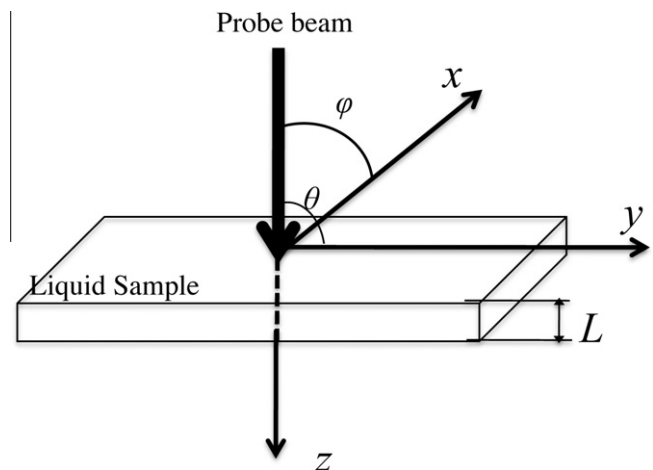


Fig. 2. Schematic diagram of computational domain.

$$y = \frac{n_0[\exp(kz/n_0) - 1]^2}{2k \exp(kz/n_0)} \quad (9)$$

and refractive angle can be obtained as:

$$\alpha = \frac{dy}{dz} = \frac{1}{2} \exp\left(\frac{kz}{n_0}\right) - \frac{1}{2} \exp\left(-\frac{kz}{n_0}\right) \quad (10)$$

Eq. (10) shows the expression of the refractive angle as a function of the temperature gradient and the thickness of the liquid medium (optical path length). Fig. 3 shows the relationship between refractive angle and temperature gradient at points where the thickness of liquid medium, L , is 1.5, 3.0 and 4.5 mm respectively. As shown in Fig. 3 the relationship between refractive angle and temperature gradient can be well approximated as linear at a small temperature gradient.

4. Experimental set-up

Fig. 4 shows the experimental set-up to measure the refractive angle. Fluidic optical device in Fig. 4 is a Pyrex vessel (internal size: $21 \times 10 \times L$ [mm]), thickness of the liquid medium, L , can be varied) filled with ethylene glycol. The vessel is held in an adiabatic material (Mica glass–ceramics (Photoveel®)) as shown in Fig. 5. The temperature on both sides of the vessel was controlled by a heater–heat sink system to create a one-dimensional temperature distribution in the liquid medium.

Fig. 6 shows the experiment set up to measure the temperature distribution in the liquid sample. The thermocouples (K-type, 1 mm diameter) are located at 5 points with 2 mm pitch in the upper surface of the vessel and immersed 1 mm in the liquid sample.

The temperature gradient in the experiment is given as:

$$\frac{dT}{dy} = \frac{T_4 - T_5}{\Delta y} \quad (11)$$

In which, Δy is the distance between two thermocouples to obtain the temperature gradient, $\Delta y = 4$ mm.

A CW laser ($P = 0.6$ mW, $\lambda = 632$ nm, $\Phi = 0.8$ mm, TEM₀₀) is used as a probe beam. A CCD camera (OPHIR, BeamStar-FX 50) is used as a detector. Based on probe beam position, the refractive angle is estimated.

$$\alpha = \frac{r}{d} \quad (12)$$

where, d is the distance from the experiment section to the detector of the camera, $d = 286$ mm; r is the beam position.

5. Results and discussion

Fig. 7(a and b) show the comparison of theoretical and experimental results at points where the thickness of liquid medium, L ,

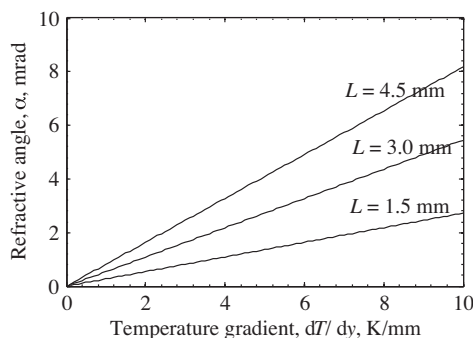


Fig. 3. Refractive angle as a function of temperature gradient.

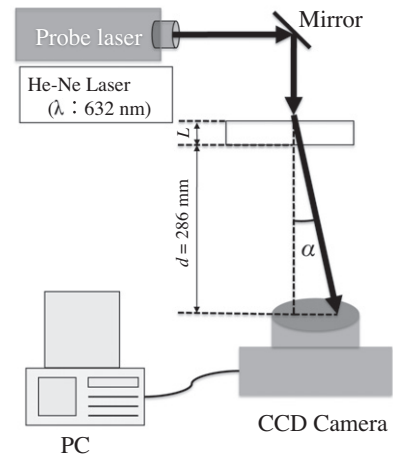


Fig. 4. Refractive angle measurement system.

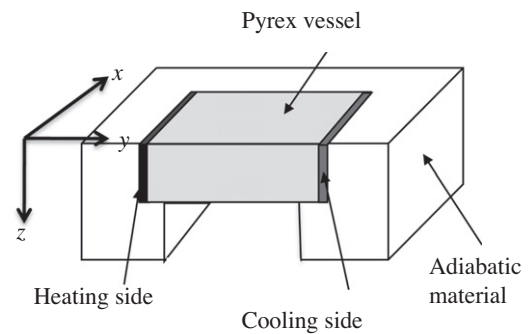


Fig. 5. Schematic diagram of sample.

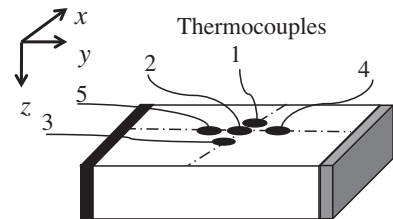
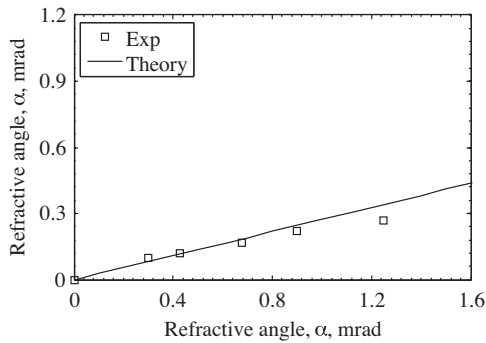


Fig. 6. Temperature gradient measurement system.

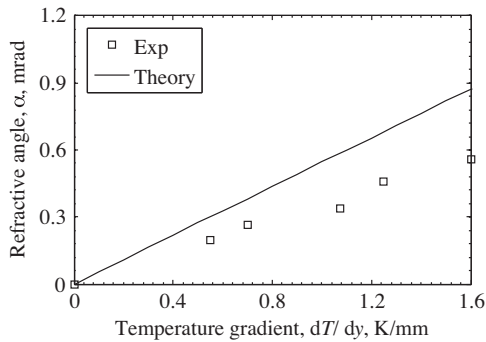
is 1.5, 3.0 mm respectively. The temperature gradient in the experimental results is based on the measurement as described above. As shown in this figure, theoretical and experimental results agree well with each other. The experimental data includes the error corresponding to the difference between the actual temperature gradient at the laser incidence and that is calculated by using Eq. (11). The discrepancy at higher dT/dy may correspond to the error where the measured temperature gives higher dT/dy and therefore higher a prediction by using Eq. (10). This discrepancy should increase with increasing sample thickness and the temperature gradient. The effect of natural convection is considered in the following section.

6. Calculation of the temperature field

Fig. 8 shows the calculation domain, consists of glass and the liquid sample, ethylene glycol. The thickness of the upper glass is different with the one of the lower glass following the scale of



(a) $L = 1.5$ mm



(b) $L = 3$ mm

Fig. 7. The comparison of theoretical and experimental results.

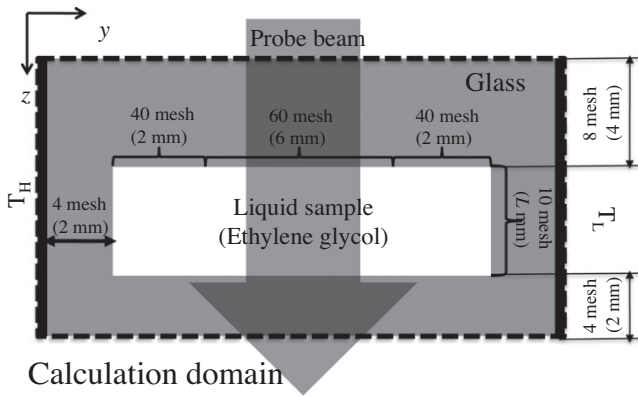


Fig. 8. The calculation domain.

the real cuvette. Here, the upper glass layer is designed thicker to give nuts (in a hole to fill the liquid sample in and out of the cuvette) a few screws. The thermal conductivity of glass and ethylene glycol is shown in Table 1. The regions, which are near the boundary between liquid and glass walls are divided by a fine mesh. And another regions are divided by more coarse size of mesh as shown in Fig. 8.

Table 1
Calculation conditions.

Parameter	(a)	(b)
Temperature of heating side, °C	46	47.5
Temperature of cooling side, °C	16	17.5
Thermal conductivity of glass, W/(m K)	1.26	1.26
Thermal conductivity of ethylene glycol, W/(m K)	0.26	0.26

To consider the natural convection effect, the temperature distribution of liquid sample in steady state is calculated numerically following these governing equations [14]:

$$v \frac{\partial v}{\partial y} + w \frac{\partial w}{\partial z} = 0 \quad (13)$$

$$v \frac{\partial v}{\partial y} + w \frac{\partial w}{\partial z} = -\frac{1}{\rho} \frac{\partial p}{\partial y} + \nu \left(\frac{\partial^2 v}{\partial y^2} + \frac{\partial^2 v}{\partial z^2} \right) \quad (14a)$$

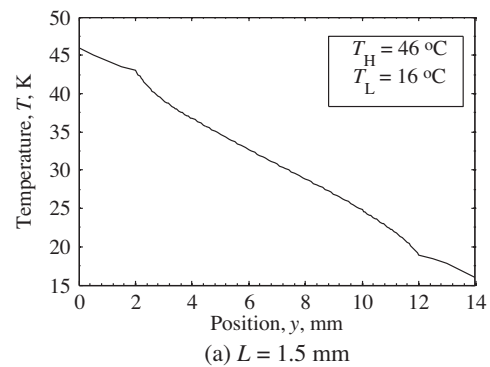
$$v \frac{\partial w}{\partial y} + w \frac{\partial w}{\partial z} = -\frac{1}{\rho} \frac{\partial p}{\partial z} + \nu \left(\frac{\partial^2 w}{\partial y^2} + \frac{\partial^2 w}{\partial z^2} \right) - g\beta(T - T_0) \quad (14b)$$

$$v \frac{\partial T}{\partial y} + w \frac{\partial T}{\partial z} = a \left(\frac{\partial^2 T}{\partial y^2} + \frac{\partial^2 T}{\partial z^2} \right) \quad (15)$$

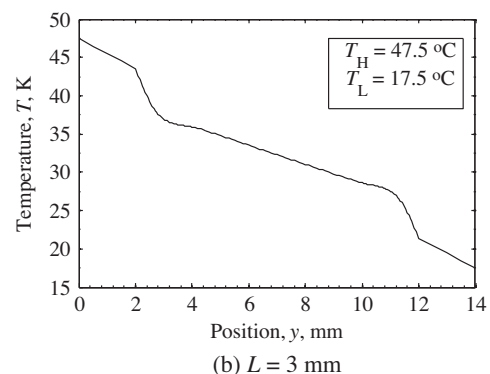
In the motion equation, the buoyant force is expressed as a function of the temperature, therefore the natural convection is a result of temperature variation, and there is only density change by temperature variation as expressed in the Boussinesq approximation.

The temperature distribution is calculated numerically base on finite difference method. The 1st order upwind scheme and a center 2nd order are applied for discretize the advection term and the diffusion term respectively.

Fig. 9(a and b) show the calculated temperature distribution along the y -axis at points where the thickness of the liquid medium, L , is 1.5, 3.0 mm respectively. When compared with the case of calculation by one-dimensional heat conduction model (consists of glass and liquid sample), the temperature gradient along the y -axis, calculated by 2-dimensional natural convection heat transfer model, is smaller and the difference is about 35%, which cannot be ignored for predictions. In addition the heating and cooling side are separated from the liquid sample by the glass walls, which perturb the temperature gradient. For the improvement of the device, the



(a) $L = 1.5$ mm



(b) $L = 3$ mm

Fig. 9. The temperature distribution along the y -axis.

thinner and higher heat conduction heating and cooling walls are required to predict the device function more easily.

Because of the effect of natural convection, the measured temperature gradient has a marginal error between thermocouples 4 and 5, Δy , is long, and it can be expressed as a function of Δy as:

$$\text{error} = \frac{\left(\frac{dT}{dy}\right)_c - \frac{T_1 - T_r}{\Delta y}}{\left(\frac{dT}{dy}\right)_c} \quad (16)$$

where, $(dT/dy)_c$ is the temperature gradient calculated numerically. And T_1 and T_r are calculated temperature at 2 points on the y -axis and distance $\Delta y/2$ from the center in left and right side respectively.

By changing Δy one can obtain the relationship between the temperature gradient error and the distance between two thermocouples to obtain the temperature gradient shown in Fig. 9(a and b). As shown in Fig. 10(a and b), the temperature gradient error increases with the increasing distance between two thermocouples to obtain the temperature gradient due to the temperature distribution. Therefore, the actual temperature gradient at the laser incidence is larger than that calculated by using Eq. (11). However, the error is very small (smaller than 3%) and one can ignore it.

Fig. 11(a and b) show the temperature distribution along the z -axis at points where the thickness of the liquid medium, L , is 1.5, 3.0 mm respectively. Because of the natural convection, fluid motion is characterized by a recirculating flow for which fluid ascends along the heating wall and descends along the cooling wall. As a consequence, temperature of the upper glass layer is higher than the one of the lower glass layer. In glass domain the temperature is increasing along the z -axis. On the other hand, in the liquid sample domain, the temperature is decreasing along the z -axis. Compared with the the-

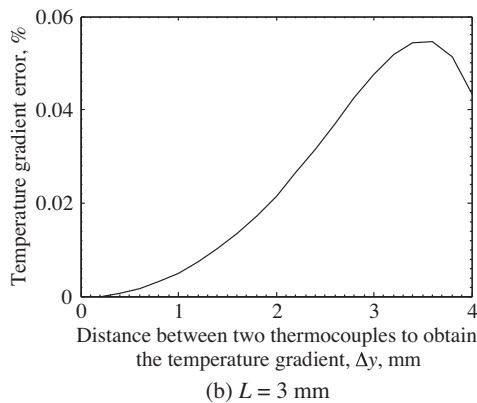
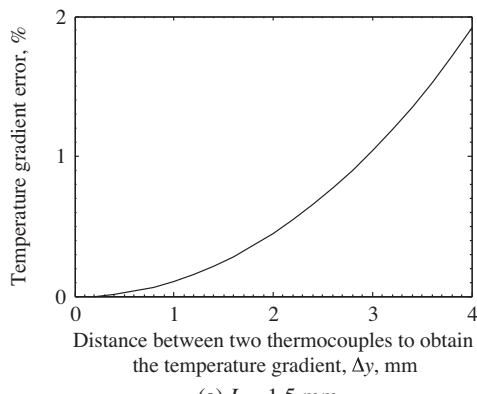


Fig. 10. The temperature gradient given by Eq. (11) as a function at the distance of thermocouples 4 and 5.

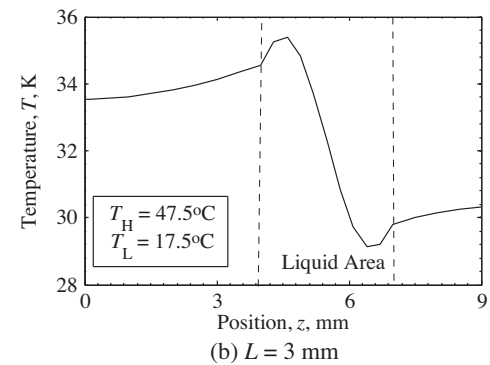
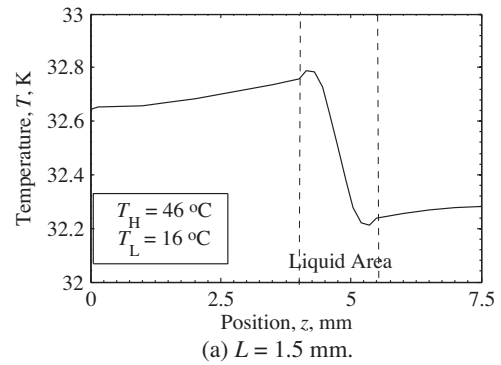


Fig. 11. The temperature distribution along the z -axis.

oretical refractive angle, the experimental refractive angle has a marginal error, corresponding to the temperature distribution along the z -axis. Therefore, it is necessary to calculate the ray trace of the probe beam in the case it passes through a two-dimensional temperature distribution in order to consider the effect of the temperature distribution along the z -axis.

The model shown in Fig. 12 is considered. The liquid medium has a two-dimensional refractive index distribution in the y and z -axis. The refractive index can be expressed as a function of the temperature as:

$$n(T) = n_0 + \frac{dn}{dT} \times (T - 25) \quad (17)$$

where, n_0 is the refractive index of ethylene glycol at 25 °C.

Applying the Euler-Lagrange method to Fermat's principle, the ray trajectory equation can be written as [15,16]:

$$\frac{d}{ds} \left(n(y,z) \frac{dR}{ds} \right) = \text{grad}(n) \quad (18)$$

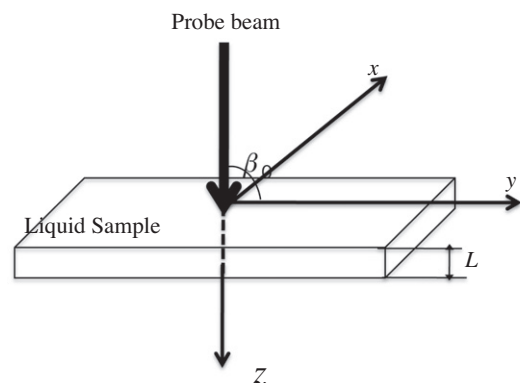


Fig. 12. The 2-dimensional ray tracing calculation model.

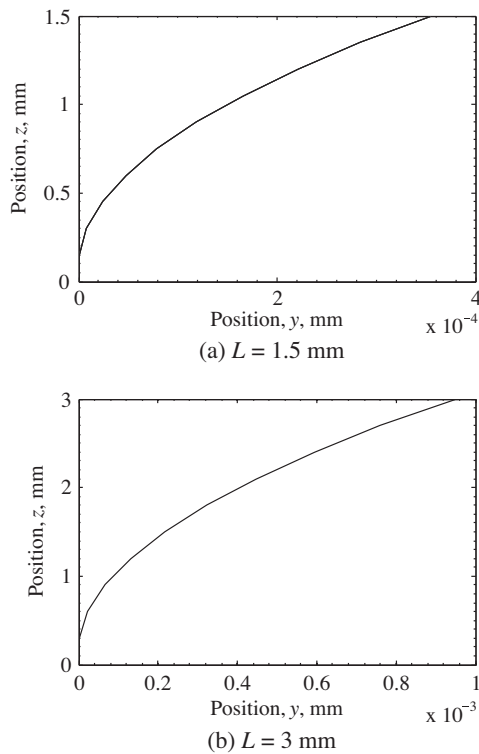


Fig. 13. The ray trajectory.

where, ds and R are the differential element of the path length and the positional vector of the ray respectively.

Numerical algorithm, equivalent to the trajectory equation, can be describe as follows [17]:

$$y_{k+1} = y_k + \Delta z \left(\frac{\cos \beta}{\cos \gamma} \right)_{k+1} \quad (19)$$

$$ds_{k+1} = \frac{\Delta z}{(\cos \gamma)_{k+1}} \quad (20)$$

where, Δz is the elementary step along the z -axis and $[\cos \beta, \cos \gamma]$ is the unit directional vector, which is calculated in successive integration steps:

$$(\cos \beta)_{k+1} = (\cos \beta)_k + \left[\frac{1}{n} (n_y - (n_y \cos \beta + n_z \cos \gamma) \cos \beta) ds \right]_k \quad (21)$$

$$(\cos \gamma)_{k+1} = \sqrt{1 - (\cos^2 \beta)_{k+1}} \quad (22)$$

$$(n_y, n_z) = \text{grad}(n) \quad (23)$$

When the incident angle, β_0 , is $\pi/2$, the ray trajectory can be obtained as shown in the Fig. 13(a and b). In the case of liquid medium's thickness is 1.5 mm, the refractive angle is 0.471 mrad. When compared with the refractive angle calculated by using one-dimensional model (0.522 mrad), the difference between them is 10%. However, in the case of liquid medium's thickness is 3.0 mm, the refractive angle is 0.626 mrad. When compared with the refractive angle calculated by using one-dimensional model (0.779 mrad), the error is about 20% and one cannot ignore it.

Therefore one cannot ignore the effect of the temperature distribution in the z -axis in the case of large liquid medium's thickness. The discrepancy becomes larger by increasing the sample thickness and the temperature gradient that may appear in actual application situation.

7. Conclusion

In this research, it is shown that the refractive angle of the probe beam, transmitted in the one-dimensional temperature distribution, is the linear function of the temperature gradient and the thickness of the liquid medium theoretically and experimentally. In the present case, it is necessary to consider the effect of natural convective heat transfer in the liquid medium. One cannot ignore the effect of the temperature distribution in the z -axis in the case of large liquid medium's thickness. The discrepancy becomes larger with increasing of the liquid medium and the temperature gradient.

In the actual application situation, a small liquid medium's thickness and one-dimensional model can be applied to both fluidic optical devices as an optical switching to control the light direction and a laser measurement technique to measure the thermal properties of the liquid sample which is including the temperature field and temperature diffusion coefficient. In this case, thinner and higher heat conduction heating and cooling walls are required to predict the device function more easily.

In this research, the propagation characteristic of the probe laser in one-dimensional temperature field is investigated as a basic step to develop a new model to explain the propagation characteristic of the probe laser in two-dimensional temperature field. The two-dimensional model in cylindrical coordinates is a promising tool to develop new fluidic optical devices: to predict a distance to transform the beam profile of a Gaussian beam to a flat-top and a doughnut beam in the fluidic laser beam shaper system [18,19]; to calculate the focal length of the fluidic lens [20].

Acknowledgements

Part of this work has been supported by the Grant-in-Aid for Scientific Research (19360095) of MEXT/JSPS and by the Tokyo Tech Award for Challenging Research.

References

- [1] J.P. Gordon, R.C.C. Leite, R.S. Moore, S.P.S. Porto, J.R. Whinnery, Long-transient effects in lasers with inserted liquid samples, *J. Appl. Phys.* 36 (1965) 3–8.
- [2] S.A. Akhmanov, D.P. Krindach, A.V. Migulin, A.P. Sukhorukov, R.V. Khokhlov, Thermal self-actions of laser beams, *IEEE J. Quantum Electron.* QE-4 (1968) 568–575.
- [3] P.M. Livingston, Thermally induced modifications of a high power CW laser beam, *Appl. Opt.* 10 (1971) 426–436.
- [4] J.F. Power, Pulsed mode thermal lens effect detection in the near field via thermally induced probe beam spatial phase modulation: a theory, *Appl. Opt.* 29 (1990) 52–63.
- [5] P.P. Banerjee, R.M. Misra, M. Maghraoui, Theoretical and experimental studies of propagation of beams through a finite sample of a cubically nonlinear material, *J. Opt. Soc. Am. B* 8 (1991) 1072–1080.
- [6] J.M. Hickmann, A.S.L. Gomes, C.B. de Araújo, Observation of spatial cross-phase modulation effects in a self-defocusing nonlinear medium, *Phys. Rev. Lett.* 68 (1992) 3547–3550.
- [7] P. Govind, Agrawal, transverse modulation instability of copropagating optical beams in nonlinear Kerr media, *J. Opt. Soc. Am. B* 7 (1990) 1072–1078.
- [8] C.J. Rosenberg et al., Analysis of the dynamics of high intensity Gaussian laser beams in nonlinear de-focusing Kerr media, *Opt. Commun.* 275 (2007) 458–463.
- [9] M. Sakakura, M. Terazima, Oscillation of the refractive index at the focal region of a femtosecond laser pulse inside a glass, *Opt. Lett.* 29 (13) (2004) 1548–1550.
- [10] M. Sakakura, M. Terazima, Real-time observation of photothermal effect after photo-irradiation of femtosecond laser pulse inside a glass, *J. Phys. France* 125 (2005) 355–360.
- [11] M. Terazima, N. Hirota, S.E. Braslavsky, A. Mandelis, S.E. Bialkowski, G.J. Diebold, R.J.D. Miller, D. Fournier, R.A. Palmer, A. Tam, Quantities, terminology, and symbols in photothermal and related spectroscopies (IUPAC Recommendations 2004), *Pure Appl. Chem.* 76 (2004) 1083.
- [12] Kudou Uehara, *Basic Optics (Kougaku Kiso)* Gendaikougaku, Tokyo, Japan, 1990, pp. 45–47 (Japanese).
- [13] S.K.Y. Tang, B.T. Mayers, D.V. Vezenov, G.M. Whitesides, Optical waveguiding using thermal gradients across homogeneous liquids in microfluidic channels, *Appl. Phys. Lett.* 88 (2006) 06112.

- [14] H. Iwai, M. Haneda, T. Omura, N. Tomimura, *Simulating Thermal Fluid by Using Excel and Mouse*, Maruzen, Tokyo, Japan, (2005) (Japanese).
- [15] R.P. Feynman, R.B. Leighton, M. Sands, *The Feynman Lectures on Physics*, vol. 2, Addison Wesley Longman, 1963.
- [16] F.W. Byron, R.W. Fuller, *Mathematics of Classical and Quantum Physics*, Addison Wesley Pub. Com. Inc., 1992.
- [17] A. Grobelny, P. Powazka, J. Baczmanski, J.S. Witkowski, E.M. Beres-Pawliki, "Numerical optimization of side pump-light couplings in power lasers based on double-clad optical fibers", in: *Proceedings of the ICTON 2005*, vol. 2, 2005, pp. 355–358.
- [18] D.H. Doan, M. Chijiwa, K. Fushinobu, K. Okazaki, Investigation on the interaction among light, material and temperature field in the transient lens effect, propagation characteristics in 2D temperature field, *Therm. Sci. Eng.* 19 (2) (2011) 43–50.
- [19] D.H. Doan, Y. Akamine, K. Fushinobu, Fluidic laser beam shaper by using thermal lens effect, *Int. J. Heat Mass Transfer* 55 (2012) 2807–2812.
- [20] D.H. Doan, Y. Akamine, K. Fushinobu, Fluidic lens by using thermal lens effect, *Int. J. Heat Mass Transfer* 55 (2012) 7104–7108.